

# Correlation between substituent constants and hyperpolarizabilities for di-substituted *trans*-azobenzenes

Tsung-Yi Lin · Ajay Chaudhari · Shyi-Long Lee

Received: 9 June 2012 / Accepted: 20 August 2012 / Published online: 7 September 2012  
© Springer-Verlag 2012

**Abstract** Nonlinear optical properties of a series of disubstituted *trans*-azobenzenes were studied. The structures were fully optimized by B3LYP/6-31+G\* and both static polarizabilities and hyperpolarizabilities were then calculated by the derivative method. In order to show the relationships between dipole moments, (hyper)polarizabilities and the structures, three kinds of substituent constants were applied to correlate with both ground state dipole moment and hyperpolarizabilities. Both physical properties have a satisfactory correlation with substituent constants  $\Sigma\sigma_{+/-}$  and bond length alternation. Overall, the electronic excitation contribution to the hyperpolarizabilities is rationalized in terms of the two-level model.

**Keywords** Bond length alternation · Disubstituted *trans*-azobenzenes · NLO properties · Substituent constants

## Introduction

Significant interest exists in the design and development of materials exhibiting large second-order nonlinear optical (NLO) response because of their potential applications in telecommunications, optical computing, and

optical signal processing [1–9]. The strong oscillating electric field of laser creates a polarization response that is nonlinear and can act as a source of new optical field with altered properties [10]. The nonlinear optical susceptibilities of a material provide a quantitative measure of the ability of a bulk material to alter the optical properties and are the parameters that researchers seek to optimize. At molecular level, one can define the microscopic nonlinear coefficient (molecular hyperpolarizabilities) that is related to the bulk nonlinear optical susceptibilities. That means the NLO properties are determined by the first and second hyperpolarizabilities. To optimize optical nonlinearities at this level it is important to have a detailed discussion on the relationship between molecular electronic structure and the induced nonlinear polarization. The focus of research in this field has been on donor-acceptor-substituted  $\pi$ -conjugated molecules because the delocalized  $\pi$ -electrons give rise to the large electronic hyperpolarizabilities.

Early study of the structure–property relationships of these molecules indicated that the  $\beta$  increases with an increase in donor and acceptor strength and with extending  $\pi$ -conjugation length [3, 11]. Oudar reported that for mono-substituted *trans*-stilbene derivatives, the  $\beta$  values are typically ten times larger than the benzene compounds [12]. The other factor is the intramolecular charge transfer occurring within the donor-acceptor disubstituted  $\pi$ -conjugated systems. In addition to the two factors described above, there is another important factor that potentially affects the magnitude of  $\beta$  values. This factor is nothing but  $\pi$ -electron bridge, which connects the two benzene rings. In order to obtain the large  $\beta$  values, the  $\pi$ -electron donating power of the donor groups should be transferred effectively to the acceptor groups through long  $\pi$ -conjugated systems. As a result, the  $\pi$ -electron-transfer efficiency depends on the electronic nature of the bridge.

T.-Y. Lin · S.-L. Lee (✉)

Department of Chemistry and Biochemistry, National Chung Cheng University,  
ChiaYi 621, Taiwan  
e-mail: chesll@ccu.edu.tw

A. Chaudhari (✉)

Department of Physics, The Institute of Science, FORT,  
Mumbai 400032, India  
e-mail: ajaychau5@yahoo.com

Singer et al. measured the  $\beta$  values of a series of organic  $\pi$ -conjugated molecules, including some stilbene, imine, and azobenzene derivatives, using dc-induced second-harmonic generation (DCSHG) [13]. They found that  $\beta$  values of stilbene and azobenzene derivatives are essentially the same, indicating that there are only minor differences between the transition dipole moments of the ethylenic and azo bridges, with the validity of the two-level charge-transfer model [14]. Ulman applied the Hammett ( $\sigma_p$ ), Brown-Okamoto ( $\sigma^+$ ), and Biggs-Robinson ( $\sigma^-$ ) constant to correlate with the ground state dipole moments and hyperpolarizabilities [15]. The result showed that the Hammett constant has a good correlation with both ground state dipole moments and hyperpolarizabilities. Similar correlations were not obtained for the azobenzenes.

The azobenzene in which the N=N links the two phenyl rings, has potential applications in molecular switches and therefore it was studied both theoretically as well as experimentally [16–27]. Recently, it has been shown that certain azobenzene derivatives have some novel properties and potential applications [28–41]. The present work is intended for the understanding of the molecular structure-NLO properties relationships of azobenzenes with common donor-acceptors of a variety of strengths. Various computational methods with different basis sets were applied to show the bridge structure of azobenzene and compare it with experimental data. Three different substituent constants are then used as parameters to correlate with ground state dipole moments and hyperpolarizabilities of azobenzene derivatives.

## Calculation methods

The *trans*-azobenzenes (TAB) optimized structures were carried out by MP2, HF [42] and density functional theory (B3LYP [43] functional, Gaussian 03 program package [44]). To study the effect of basis set on stability of TAB, we optimized the structures with two basis sets viz. 6-31+G\*, 6-31G\*\*. It is noted that the choice of basis set is critical for obtaining the stable structures. The 6-31+G\* basis set that includes the diffuse functions is essential for accurately describing the interaction between the two phenyl rings in TAB. The ground-state structure has been determined by a standard force-minimization process, and the vibrational spectrum has been systematically determined to check that all the vibrational frequencies are real. The static hyperpolarizabilities are calculated using derivative method which relates different derivatives of energy or dipole moment to various coefficients of power series expansions. Here we adopt the energy expression to get

the linear and NLO coefficients.

$$U(E) = U^0 - \sum_i \mu^0 E_i - \frac{1}{2} \sum_{ij} \alpha_{ij} E_i E_j - \frac{1}{3} \times \sum_{ijk} \beta_{ijk} E_i E_j E_k - \frac{1}{4} \sum_{ijkl} \gamma_{ijkl} E_i E_j E_k E_l \quad (1)$$

$$\alpha_{ij} = \left. \frac{\partial U^2(E)}{\partial E_i \partial E_j} \right|_{E=0} \quad (2)$$

$$\beta_{ijk} = \left. \frac{\partial^3 U(E)}{\partial E_i \partial E_j \partial E_k} \right|_{E=0} \quad (3)$$

$$\gamma_{ijkl} = \left. \frac{\partial^4 U(E)}{\partial E_i \partial E_j \partial E_k \partial E_l} \right|_{E=0} \quad (4)$$

where  $U^0$  is the energy of molecule in absence of an electric field;  $\mu^0$  is the components of the dipole moment vector;  $\alpha$  is the linear polarizability tensor;  $\beta$  and  $\gamma$  are the second- and third- polarizability tensor, respectively; and i, j, k label the x, y, and z components, respectively. Numerically  $\beta_{xxx}$  can be calculated as:

$$\beta_{xxx} = \{-E(2F_x) + E(-2F_x) + 2[E(F_x) - E(-F_x)]\} / 4(F_x)^3 \quad (5)$$

Here,  $E(F_x)$  indicates the total energy of a molecule in presence of a field  $F$  applied in  $x$  direction. To obtain a more intuitive description of the trends on the NLO behavior of the studied compounds, time dependent density functional theory (TDDFT) method was used to investigate the molecular electronic structures and vertical electronic excitation energies.

## Results and discussion

Stable structures of *trans*-azobenzene and computational method choice

The structure of TAB (Fig. 1) has been a subject of controversy in both experimental and theoretical study. The X-ray diffraction (XRD) [45] result showed that there was a slightly distorted but nearly planar structure of TAB. On the other hand, the gas-phase electron diffraction (ED) [46, 47] studies suggested its nonplanar structure. ED result showed that the phenyl ring was twisted by about 27.9° ( $C_i$  symmetry) around the N=N-C-C plane.

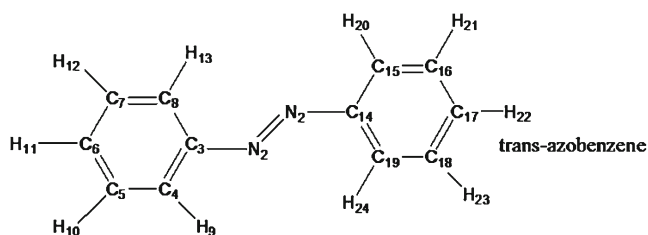


**Fig. 1** The atom numbering of TAB

Here we use different levels of theories to fully optimize TAB. Table 1 list the experimental and theoretical geometrical parameters of TAB. The optimized N=N bond length by the DFT method is closer to the ED values. The HF method underestimates both, the XRD and the ED values. The MP2 method overestimates both the experimental values. It can be seen that the N=N bond length optimized by B3LYP/6-31G\* deviates only by 0.001 Å, 0.010 Å, and 0.002 Å respectively from the three experimental ED values whereas that from the HF/6-31+G\* level deviates by 0.041 Å, 0.050, and 0.042 Å respectively. The C-N bond optimized by both, the DFT and *ab initio* methods are closer to the ED values. Especially B3LYP/6-31+G\* is consistent with ED value ( $C_2$  symmetry) of 1.420 Å. The DFT and HF methods approximately estimate the dihedral angle N=N-C-C $\sim 0^\circ$  and is comparable to the ED value. However, MP2/6-31+G\* estimates a deviation from the planarity. Kurita et al. [48] explained why the phenyl rings of TAB are significantly twisted only in the MP2/6-31+G\*.

The conformation of TAB is mainly determined by the two factors. First, the  $\pi$ - $\pi$  and  $n$ - $\pi$  interactions of the azo group with the phenyl rings and the second, the repulsive force of the ortho-hydrogens of the phenyl ring with the lone-pair electrons of the distal nitrogen. The  $\pi$ - $\pi$  interaction makes the structure favor planarity, while the repulsive and the  $n$ - $\pi$  interaction favor non-planarity. Because of the

presence of diffuse function in the 6-31+G\* basis set, the lone-pair electrons of the nitrogen atoms are described to be more localized and the  $n$ - $\pi$  interaction and repulsive force become much more important. It results in a twisted conformation of TAB. The NLO property will be maximized as the bridge is coplanar. Therefore we do not use MP2/6-31+G\* for our further calculations. On the other hand, B3LYP/6-31+G\* level estimates a little higher values of the bond lengths than the experimental values (ED) and therefore we use here B3LYP/6-31+G\* to optimize the derivatives of azo compounds in order to make a better estimation in gas phase.

### Disubstituted TAB

Thirty *trans*-azobenzenes (DTABs) selected in this study with several donor and acceptors are displayed in Fig. 2. The geometrical structures of DTABs were optimized using HF/DFT method, viz. B3LYP, with 6-31+G\* basis set. During the complete geometry optimization, all DTABs adopt the  $C_1$  point group, containing no symmetry element. The optimized parameters, i.e., bond lengths and bond angles of DTABs computed using B3LYP with the 6-31+G\* basis set are presented in Table 2. We have used -NO<sub>2</sub>, -COCH<sub>3</sub>, -COH, -COCl, -CN, -CF<sub>3</sub> as the acceptor groups, and -CH<sub>3</sub>, -OH, -OMe, -NH<sub>2</sub>, -NMe<sub>2</sub> as the donors. The acceptor and donor groups are attached in the 11 and 22 position, respectively.

We present a comparative study of the N=N and C-N bond lengths, N=N-C angle, C-N=N-C, N=N-C-C dihedral angles in TAB and DTABs. We first discuss the substitution effect on the structural parameters of TAB. From Tables 1 and 2, it can be seen that in all substituted TABs, the N=N bond length is longer than that in the nonsubstituted TABs. Especially in molecules 1e, 2e, 3e, 4e, 5e, and 6e, the N=N bond length increases by 0.009, 0.008, 0.008, 0.008, 0.007 and 0.009 Å, respectively than TAB. Interestingly, a reverse trend is observed for the C-N bond distance. The C-N bond

**Table 1** Structural data for *trans*-azobenzene obtained from experiments and molecular orbital calculations

	N=N	C-N	N=N-C	N-C-C	C-N=N-C	N=N-C-C <sup>a</sup>
	DFT calculations					
B3LYP/6-31G**	1.261	1.419	114.8	124.8, 115.3	-180.0	0.03
B3LYP/6-31+G*	1.258	1.420	115.3	124.7, 115.3	180.0	0.06
	HF and MP2 calculations					
HF/6-31G**	1.220	1.421	115.7	124.4, 115.5	-180.0	0.04
HF/6-31+G*	1.218	1.422	115.9	124.4, 115.5	-180.0	0.04
MP2/6-31+G*	1.278	1.423	113.6	124.3, 115.1	0.0	14.61
	Experiments					
Gas E.D. ( $C_2$ symmetry) <sup>46</sup>	1.259	1.420	116	121.2	-	30.10
Gas E.D. ( $C_i$ symmetry) <sup>46</sup>	1.268	1.427	114.5	123	-	27.90
Gas E.D. <sup>47</sup>	1.260	1.427	113.6	124.7	-	0.00
X-ray diffraction (A site) <sup>45</sup>	1.247	1.428	114.1	123.7, 115.6	-	16.70

Units: bond lengths (Å), valence and dihedral angles (degrees)

<sup>a</sup>N=N-C-C is the average value

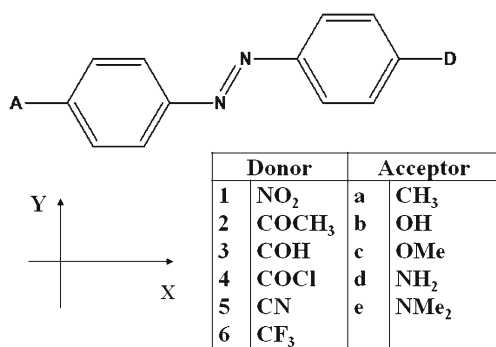


**Fig. 2** Structures of the investigated disubstituted TAB

length decreases by 0.006, 0.02, 0.021, 0.005, 0.02 and 0.006 Å in 1e, 2e, 3e, 4e, 5e and 6e, respectively, as compared to TAB. The contraction of the C-N bond and the expansion of the N=N bond in the substituted azo dyes as compared to TAB indicate a greater conjugation and  $\pi$ -

electron delocalization [49]. On the other hand, the N=N-C bond angle of molecules 1a, 1b, 1c, 1d and 1e is smaller than that for the TAB, whereas for the 2a, 2e, 3a, 3c, 4a, 4c, 5a, 5b, 5c, 6a, 6c, 6d molecules the opposite is true. If the donor group contains a methyl group, the N=N-C angle increases more than the TAB except that in 1a molecule. There is almost no change in bond angle N-N-C upon donor and acceptor substitution in TAB. It shows that the donor-acceptor groups do not affect the bond angle N-N-C.

The structural planarity maintained irrespective of the substituent. The calculated N=N-C-C dihedral angle in DTABs is similar to that of TAB except those for series 5 compounds. Especially for the 5a molecule, it shows a deviation of 1.56° from the TAB.

We now compare the geometry parameters for TAB with different donor-acceptor groups. Molecules with the same acceptor group, the N=N and C-N bond length increases and decreases respectively from the methyl

**Table 2** Optimized geometrical parameters of disubstituted *trans*-azobenzene in its ground state

Molecule	N=N	C-N	N=N-C	N-C-C	C-N=N-C	N=N-C-C
1a	1.260	1.419	114.7	124.7, 115.3	-180	0.07
1b	1.262	1.418	114.7	124.8, 115.4	-180	0.20
1c	1.263	1.418	114.6	124.8, 115.4	-180	0.04
1d	1.265	1.415	114.5	124.8, 115.5	180	0.20
1e	1.267	1.414	114.5	124.9, 115.5	-180	0.01
2a	1.260	1.414	115.4	124.9, 115.7	180	0.11
2b	1.261	1.418	115.0	124.9, 115.5	-180	0.01
2c	1.262	1.418	114.9	124.9, 115.6	-180	0.01
2d	1.264	1.417	114.8	124.9, 115.6	-180	0.50
2e	1.266	1.400	115.9	125.4, 116.3	180	0.32
3a	1.260	1.413	115.5	124.9, 115.6	180	0.01
3b	1.262	1.418	114.9	124.7, 115.3	180	0.01
3c	1.262	1.407	115.7	125.1, 115.8	-180	0.05
3d	1.264	1.416	114.8	124.8, 115.4	180	0.29
3e	1.266	1.399	115.0	125.4, 116.3	180	0.02
4a	1.260	1.413	115.6	124.9, 115.6	-180	0.03
4b	1.261	1.418	114.8	124.8, 115.4	-180	0.02
4c	1.262	1.407	115.8	125.0, 115.8	-180	0.01
4d	1.264	1.401	116.0	125.2, 116.0	180	0.14
4e	1.266	1.415	114.6	124.9, 115.6	-180	0.00
5a	1.259	1.414	115.5	124.9, 115.6	-180	1.60
5b	1.261	1.409	115.7	125.0, 115.7	-180	1.00
5c	1.261	1.408	115.7	125.1, 115.7	-180	1.23
5d	1.263	1.418	114.7	124.8, 115.6	180	1.01
5e	1.265	1.400	116.0	125.4, 116.3	-180	0.83
6a	1.260	1.419	114.7	124.8, 115.4	-180	0.00
6b	1.262	1.418	114.7	124.9, 115.4	-180	0.06
6c	1.263	1.405	115.7	125.1, 115.7	180	0.07
6d	1.265	1.400	116.0	125.2, 116.0	180	0.51
6e	1.267	1.414	114.6	125.0, 115.6	180	0.06

group donor substituted molecule (1a, 2a, 3a, 4a, 5a, 6a) to dimethylamino group donor substituted molecule (1e, 2e, 3e, 4e, 5e, 6e). Molecules with the same acceptor group, the bond length C-N decreases from the methyl substituted molecule (1a, 2a, 3a, 4a, 5a, 6a) to dimethylamino substituted molecule (1e, 2e, 3e, 4e, 5e, 6e). Earlier work by Biswas and Umapathy also showed that the substituted group may affect the geometry parameter [50]. Also the well known resonance [49] and inductive effect [51, 52] may appropriately explain the relationship between donor-acceptor groups and the geometry. For example, in series 1 DTAB, the donor group changes from methyl group to dimethylamino group. The dimethylamino group can easily donate electrons to the bridge and act as a strong donating group. Also the nitro group can withdraw the electrons from the bridge. Due to this effect, the  $\pi$ -electron may become more delocalized so that the bond length N=N

becomes elongated and the C-N bond length shortened. On the other hand, the calculated C-N=N-C dihedral angle is independent of donor-acceptor effect. The N=N-C-C dihedral angle in DTABs is smaller than  $1^\circ$ , except for 5a, 5b, 5c, 5d molecules.

#### Correlation between dipole moments and hyperpolarizabilities with substituent constants

The calculated dipole moments, (hyper) polarizabilities and substituent constants for disubstituted azobenzenes are presented in Table 3. The substituent effect is presented by the difference of the individual substituent constants, Eq. 6,

$$\sum \sigma = \sigma(\text{D}) - \sigma(\text{A}), \quad (6)$$

where acceptor and donor are the substituent on the 11 and 22 positions respectively (Fig. 1). The Hammett

**Table 3** Calculated longest wavelength absorption maxima, dipole moments, (hyper) polarizabilities, and substituent constants of DTABs

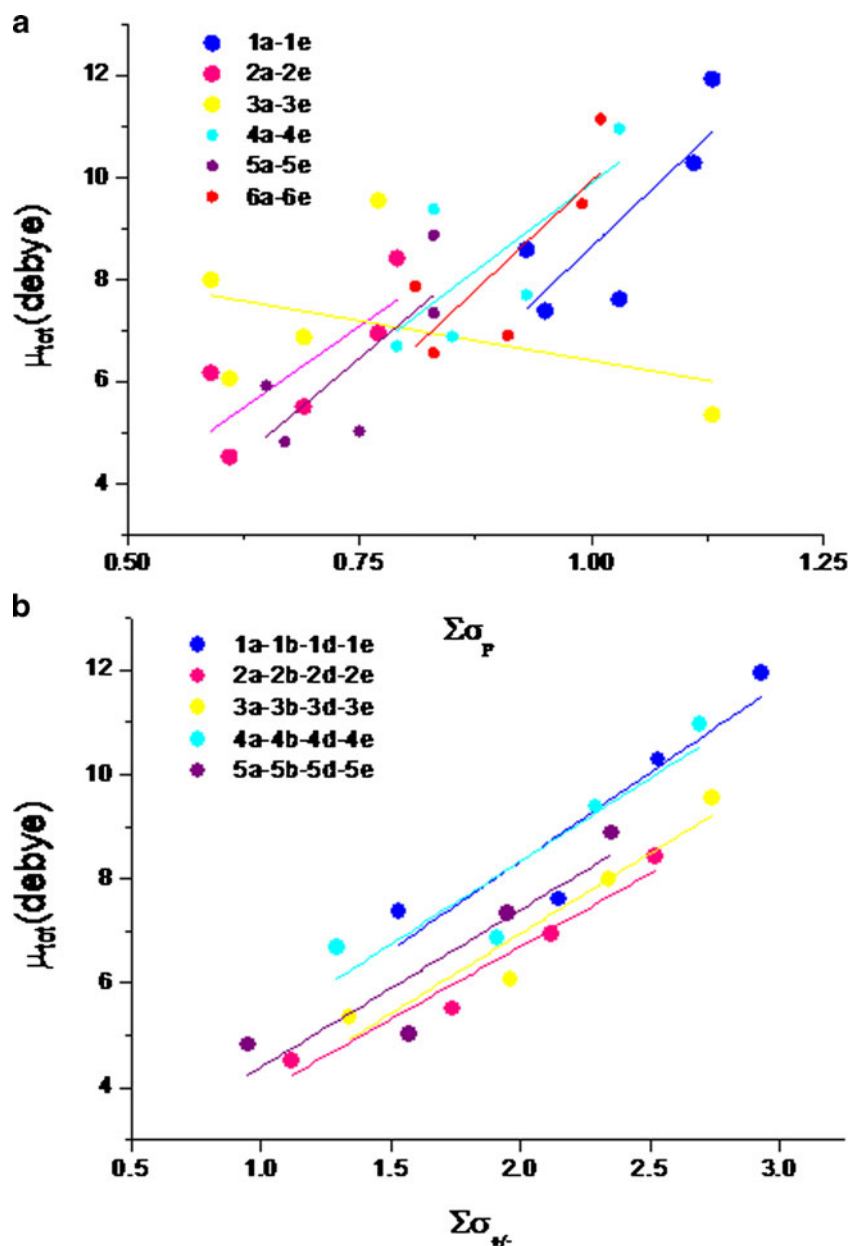
Molecule	$\lambda_{\text{max}}$	$\mu_{\text{tot}}$	$\alpha_{\text{xx}}$	$\alpha_{\text{ave}}$	$\beta_{\text{xxx}}$	$\Sigma\sigma_{\text{p}}^{53}$	$\Sigma\sigma_{+/-}^{53}$
1a	381	7.38	63.08	34.55	64.96	0.95	1.53
1b	397	7.61	63.47	34.01	87.72	1.03	2.15
1c	406	8.59	69.49	36.91	106.64	0.93	2.01
1d	432	10.28	71.81	37.12	133.90	1.11	2.53
1e	465	11.93	85.83	43.79	200.06	1.13	2.93
2a	364	4.53	64.51	35.86	39.06	0.61	1.12
2b	375	5.51	64.37	35.15	55.18	0.69	1.74
2c	381	6.17	70.04	37.93	68.56	0.59	1.6
2d	401	6.95	71.37	37.83	87.84	0.77	2.12
2e	429	8.42	84.22	44.12	135.94	0.79	2.52
3a	368	5.35	62.95	34.27	44.09	1.13	1.34
3b	380	6.06	62.99	33.60	60.38	0.61	1.96
3c	387	6.87	68.78	36.42	74.85	0.69	1.82
3d	407	7.99	70.27	36.38	94.34	0.59	2.34
3e	435	9.55	83.34	42.75	144.27	0.77	2.74
4a	361	6.69	68.84	34.28	27.65	0.79	1.29
4b	372	6.88	63.72	33.57	42.10	0.85	1.91
4c	383	7.69	68.80	36.24	54.29	0.93	1.77
4d	397	9.38	70.65	36.22	70.13	0.83	2.29
4e	423	10.95	83.33	42.45	111.40	1.03	2.69
5a	348	4.82	56.61	32.39	20.23	0.67	0.95
5b	360	5.03	56.26	31.60	32.03	0.75	1.57
5c	365	5.92	61.59	34.28	41.69	0.65	1.43
5d	384	7.34	62.37	33.99	53.44	0.83	1.95
5e	409	8.87	74.05	39.89	85.87	0.85	2.35
6a	372	6.56	66.53	36.69	10.80	0.83	–
6b	385	6.90	66.77	36.10	12.37	0.91	–
6c	393	7.86	72.73	39.01	24.23	0.81	–
6d	415	9.48	74.94	39.16	44.36	0.99	–
6e	445	11.14	88.88	45.80	98.26	1.01	–

Units: wavelength absorption maxima (nm), dipole moment (debye), polarizabilities( $10^{-24}$  esu), hyperpolarizabilities( $10^{-30}$  esu)

constant was evaluated from the effect which the substituent has on the ionization of benzoic acids [53]. Brown and Okamoto utilized the solvolysis of  $\alpha$ -cumyl chloride in 90 % acetone-water as a standard for defining  $\sigma^+$  constants (i.e., for reactions in which a full positive charge is developed), and thus the electron demand on the substituent is so strong that the resonance contribution of this substituent is greater than the usual [54]. A similar procedure was used by Biggs and Robinson to define  $\sigma^-$  constants using the ionization of phenols as a standard reaction, i.e., when the electron withdrawing ability of a substituent is large enough and can not be described by the usual resonance interaction [55].

In Fig. 3, the plots of the dipole moments as a function of  $\Sigma\sigma_p$  and  $\Sigma\sigma_{+/-}$ , are presented. While in the case of  $\Sigma\sigma_{+/-}$  the results fit the line with a correlation coefficient of 0.92 (or higher), the other one has a correlation coefficient of 0.81 (or lower). Ulman showed that the Hammett substituent constant consists of both inductive and resonance effects and both the effects are important to the molecules [15]. On the other hand, the  $\sigma_+$  and  $\sigma_-$  constants push the resonance effects to their extreme, while giving the inductive effect less influence. In DTAB series 1, 2, 3, 4, and 5 donor group change from methyl group to dimethylamino group, i.e., the donor ability is increasing in this

**Fig. 3** Calculated ground state dipole moments of DTABs **a** as a function of  $\Sigma\sigma_p$  **b** as a function of  $\Sigma\sigma_{+/-}$



series. The donor group will easily push electrons to the bridge and remain itself positively charged. This situation may affect the magnitude of dipole moments. The greater the charge separation the higher the dipole moment. As a result, there may be a better correlation of dipole moments with  $\Sigma\sigma_{+/-}$ .

In Fig. 4a and b the  $\beta_{xxx}$  values are plotted as a function of  $\Sigma\sigma_p$  or  $\Sigma\sigma_{+/-}$  respectively. Linear correlations are found between all three substituent constants and  $\beta_{xxx}$  with a better fit in the case of  $\Sigma\sigma_{+/-}$  ( $r=0.94$ ). It can be seen that the variety of donor groups having different electron donating abilities affect the magnitude of static hyperpolarizabilities of DTABs. As the magnitude of  $\Sigma\sigma_{+/-}$  increases, the donor abilities as well as the polarizabilities increase.

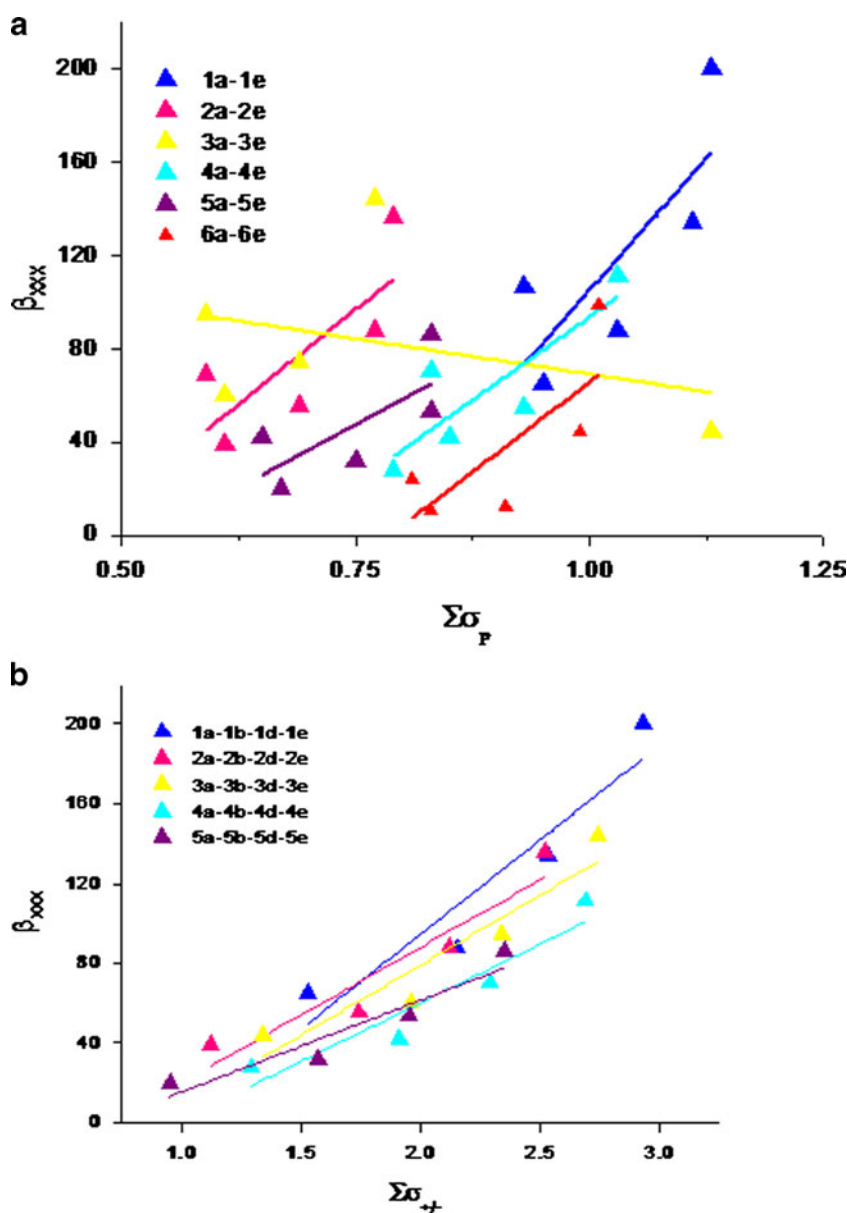
Two level model and electronic properties with hyperpolarizabilities

On the basis of the complex sum over states (SOS) expression, Oudar and Chemla established a simple link between  $\beta$  and low-lying charge-transfer transition through the two-level model [12, 14]. The static first hyperpolarizability is expressed by the following expression:

$$\beta \propto (\mu_{ee} - \mu_{gg}) \frac{\mu_{ge}^2}{E_{ge}^2}, \tag{7}$$

where  $\mu_{ee}$  and  $\mu_{gg}$  are the ground state and excited-state dipole moment,  $\mu_{ge}$  is the transition dipole, and  $E_{ge}$  is the transition energy. One can estimate these quantities using

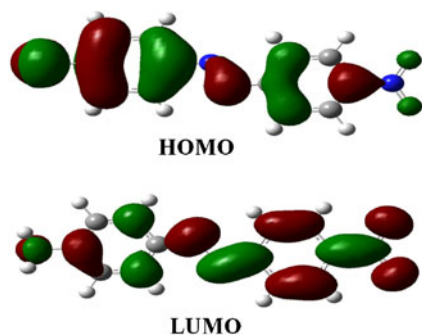
**Fig. 4** Calculated ground state hyperpolarizabilities of DTABs **a** as a function of  $\Sigma\sigma_p$  **b** as a function of  $\Sigma\sigma_{+/-}$



**Table 4** Results of TDDFT calculations at B3LYP/6-31+G\* level for the electron transitions of all molecules

Molecule	$\beta_{xxx}$	$E_{ge}$ (eV)	$\mu_{ge}^2$	$\mu_{ge}^2/E_{ge}^2$
1a	64.96	3.25	0.889	0.084
1b	87.72	3.12	0.853	0.088
1c	106.64	3.06	0.888	0.095
1d	133.90	2.87	0.846	0.103
1e	200.06	2.67	0.882	0.124
2a	39.06	3.41	1.022	0.088
2b	55.18	3.30	0.999	0.092
2c	68.56	3.25	1.054	0.100
2d	87.84	3.09	1.015	0.106
2e	135.94	2.89	1.0603	0.127
3a	44.09	3.37	1.007	0.089
3b	60.38	3.26	0.982	0.092
3c	74.85	3.21	1.034	0.100
3d	94.34	3.05	0.997	0.107
3e	144.27	2.85	1.043	0.128
4a	27.65	3.44	1.029	0.087
4b	42.10	3.33	1.007	0.091
4c	54.29	3.24	0.993	0.095
4d	70.13	3.12	1.029	0.106
4e	111.40	2.93	1.081	0.126
5a	20.23	3.56	0.903	0.071
5b	32.03	3.45	0.886	0.074
5c	41.69	3.39	0.947	0.082
5d	53.44	3.23	0.916	0.088
5e	85.87	3.03	0.975	0.106
6a	10.8	3.34	1.031	0.092
6b	12.37	3.22	1.006	0.097
6c	24.23	3.16	1.055	0.106
6d	44.36	2.99	1.023	0.114
6e	98.26	2.79	1.072	0.138

the TDDFT method. These quantities are presented in Table 4. Hence, as a guideline, the two-level model requires well-performing NLO chromophores that possess a low-lying CT excited state with large oscillator strength [56].

**Fig. 5** The HOMO and LUMO of 1d molecule

The enhancement of  $\beta$  values with increasing donor-acceptor abilities can be attributed to the increasing  $\mu_{ge}^2$  and decreasing  $E_{ge}$  values. The results show that the trend of  $\mu_{ge}^2/E_{ge}^2$  values is  $1e > 1d > 1c > 1b > 1a$  and is in agreement with the  $\beta_{xxx}$  values. On comparing the -OH and -NH<sub>2</sub> substituted molecules (1b, 1d) with the methyl substituted molecules (1a), it is found that 1d compound possess smaller  $\mu_{ge}^2$  value. However, the static hyperpolarizability of the -NH<sub>2</sub> substituted molecule (1d) is twice that of the methyl substituted molecules.

Figure 5 shows the HOMO and LUMO for the 1d molecule. The transition energy of 1d is found to be smaller than 1a (0.38 eV). The contribution of the square form to the two-level model dominates the major effect to the hyperpolarizability. Besides the transition energy, there may be other reasons to affect the hyperpolarizability of 1d molecule. The first electronic transition is primarily composed of the HOMO-LUMO transition. As the methyl group is replaced

**Table 5** Evolution of hyperpolarizabilities as a function of the BLA for DTABs

Molecule	BLA	$\beta_{xxx}$
1a	0.159	64.96
1b	0.156	87.72
1c	0.155	106.64
1d	0.150	133.90
1e	0.147	200.06
2a	0.154	39.06
2b	0.157	55.18
2c	0.156	68.56
2d	0.153	87.84
2e	0.134	135.94
3a	0.153	44.09
3b	0.156	60.38
3c	0.145	74.85
3d	0.152	94.34
3e	0.133	144.27
4a	0.153	27.65
4b	0.157	42.10
4c	0.145	54.29
4d	0.137	70.13
4e	0.149	111.40
5a	0.155	20.23
5b	0.148	32.03
5c	0.147	41.69
5d	0.155	53.44
5e	0.135	85.87
6a	0.159	10.8
6b	0.156	12.37
6c	0.142	24.23
6d	0.135	44.36
6e	0.147	98.26

Units: BLA (Å), hyperpolarizabilities ( $10^{-30}$  esu)



by the  $-NH_2$ , the HOMO energy is higher and the LUMO energy does not change significantly. The electron density of the HOMO orbital, which is confined more to the electron-donating group ( $-NH_2$ ), would favor the charge transfer to the LUMO orbital, confined toward the acceptor part ( $-NO_2$ ) of a molecule. Clearly, the excitation mostly consists of CT from the donor group to the acceptor group. This condition also occurs in other series (comparing 2a vs. 2d, 3a vs. 3d, 4a vs. 4d, 5a vs. 5d, 6a vs. 6d).

A comparison of molecule 1e and 2e shows that the hyperpolarizability of 1e molecule is larger by  $64.12 \times 10^{-30}$  esu than the 2e molecule, and for the value of  $\mu_{ge}^2/E_{ge}^2$  the opposite is true. The first transition energy of 1e molecule is smaller by 0.22 eV than the 2e molecule. Equation 7 shows that the first transition energy is square order to affect the hyperpolarizability value. It again means that the first transition plays a vital role in determining the hyperpolarizability. Also comparing molecules 1e and 3e shows that the hyperpolarizability of 1e molecule is larger by  $55.79 \times 10^{-30}$  esu than the 3e molecule, and for the value of  $\mu_{ge}^2/E_{ge}^2$  the opposite is true. While the first transition energy of 1e molecule is 0.18 eV smaller than the 3e molecule, this fact has a square impact on the hyperpolarizability value. So indeed the first transition energy is really important when determining the value of hyperpolarizability.

#### Bond length alternation (BLA) with hyperpolarizabilities of DTABs

As mentioned earlier, changing the donor group from methyl group to dimethylamino group affects the N=N and C-N bond lengths. It indicates that the stronger donor strength makes the N=N bond length longer and C-N bond length shorter. In this situation, a key geometrical parameter BLA can be used to correlate with the hyperpolarizability. It is defined as the difference between the single and double bond [57, 58]. In  $\pi$ -conjugation system with disubstituted donor and acceptor groups, the increasing donor and acceptor strength follows a smaller BLA value. Hyperpolarizabilities for DTABs are presented along with BLA in Table 5.

In the first series, the hyperpolarizabilities increase from 64.96, 87.72, 106.64, 133.90 to 200.06 and the BLA values decrease from 0.159, 0.156, 0.155, 0.150 to 0.147. It shows that an increase in the strength of donor groups from methyl to dimethylamino can have a clear impact on the hyperpolarizabilities. In second series, the BLA of 2b and 2c molecules are larger than 2a molecule and so are the hyperpolarizabilities. However, the general trend is still the same as the first series. It indicates that the dimethylamino group is the strongest donor group and methyl group is the weakest in this system. In the fifth and sixth series, the trend in hyperpolarizabilities is  $5e > 5d > 5c > 5b > 5a$  and  $6e > 6d > 6c > 6b > 6a$  respectively. The corresponding BLA

sequences are  $5a = 5d > 5b > 5c > 5e$  and  $6a > 6b > 6e > 6c > 6d$ . Although there are some molecules out of the rule, the general trend is similar to the first series.

The molecules 1e, 2e, 3e, 4e, 5e have the largest hyperpolarizabilities in respective series. The trend observed for the hyperpolarizabilities is  $1e > 3e > 2e > 4e > 6e > 5e$  ( $200.06 > 144.27 > 135.94 > 111.40 > 98.26 > 85.87$ ), and that for the BLA is  $4e > 1e = 6e > 5e > 2e > 3e$  ( $0.149 > 0.147 = 0.147 > 0.135 > 0.134 > 0.133$ ). There is no good correlation between the hyperpolarizabilities and the BLA when changing the acceptor groups. The molecules 1a, 2a, 3a, 4a, 5a, 6a have the smallest hyperpolarizabilities in the respective series. The trend for the hyperpolarizabilities and BLA is  $1a > 3a > 2a > 4a > 5a > 6a$  and  $1a = 6a > 5a > 2a > 3a = 4a$  respectively. It indicates that the acceptor group has little effect on the BLA value and does not contribute to the change of hyperpolarizabilities. It can be concluded that changing the donor groups have a better effect on the BLA value and the hyperpolarizabilities in this system.

## Conclusions

We have studied the optimized TAB and a series of DTABs structures by the DFT method. The geometrical parameters optimized at B3LYP/6-31+G\* level are in agreement with the experimental determinations. The substitution of donor-acceptor group in TAB results in longer N=N bond length in DTAB than that of TAB, no matter what the substituents are. On the other hand the C-N bond length in DTABs is shorter than that in TAB. A greater conjugation and  $\pi$ -electron delocalization is built upon disubstitution of donor-acceptor substituents. Out of the three substituent constants  $\Sigma\sigma_p$ ,  $\Sigma\sigma_+$  and  $\Sigma\sigma_-$ , the  $\Sigma\sigma_+$  and  $\Sigma\sigma_-$  show a good correlation with both dipole moments as well as hyperpolarizabilities. With a change in the donor groups from methyl to dimethylamino group, the static hyperpolarizabilities become larger due to an increase in the  $\mu_{ge}^2/E_{ge}^2$  indicating that the two-level model can correctly describe the hyperpolarizability value in DTABs. The donor groups can effectively change the BLA value and hyperpolarizabilities more than the acceptor groups.

## References

1. Prasad PN, Williams DJ (1991) Introduction to nonlinear optical effects in molecules and polymers. Wiley, New York
2. Kanis DR, Ratner MA, Marks T (1994) Chem Rev 94:195–242
3. Dagani R (1996) Chem Eng News 74:22–24
4. Lindsay GA, Singer KD (1995) Polymers for second-order nonlinear optics. American Chemical Society, Washington, DC
5. Boyd DM, Kuzyk MG (1993) Polymers for electronic and photonic applications. Academic, New York

6. Peyghambarian N, Koch SW, Mysyrowicz A (1993) Introduction to semiconductor optics. Prentice Hall, Englewood Cliffs
7. Kiano T, Tomaru S (1993) *Adv Mater* 5:172–178
8. Marder SR, Perry JW (1994) *Science* 263:1706
9. Zyss J (1994) *Molecular nonlinear optics: Materials, physics and devices*. Academic, San Diego
10. Chemla DS, Zyss J (1987) *Nonlinear optical properties of organic molecules and crystals*, vol 1. Academic, New York
11. Marder SR, Sohn JE, Stucky GD (eds) (1991) *Materials for nonlinear optical: Chemical perspectives*. ACS Symposium Series 455, American Chemical Society, Washington, DC
12. Oudar JL (1977) *J Chem Phys* 67:446–457
13. Singer KD, Sohn JE, King LA, Gordon K, Dirk CW (1989) *J Opt Soc Am B* 7:1339–1350
14. Oudar JL, Chemla DS (1977) *J Chem Phys* 66:2664–2668
15. Ulman A (1988) *J Phys Chem* 92:2385–2390
16. Diau EW (2004) *J Phys Chem A* 108:950–956
17. Sauer P, Allen RE (2008) *Chem Phys Lett* 450:192–195
18. Ootani Y, Satoh K, Nakayama A, Noro T, Taketsugu T (2009) *J Chem Phys* 131:194306
19. Shao J, Lei Y, Wen Z, Dou Y, Wang Z (2008) *J Chem Phys* 129:164111
20. Cembran A, Bernardi F, Garavelli M, Gagliardi L, Oriandi G (2004) *J Am Chem Soc* 126:3234–3243
21. Ishikawa T, Noro T, Shoda T (2001) *J Chem Phys* 115:7503–7512
22. Satzger H, Sporlein S, Root C, Wachtveit J, Zinth W, Gilch P (2003) *Chem Phys Lett* 372:216–223
23. Fujino T, Tahara T (2000) *J Phys Chem A* 104:4203–4210
24. Lednev IK, Ye TQ, Abbott LC, Hester RE, Moore JN (1998) *J Phys Chem A* 102:9161–9166
25. Conti I, Garavelli M, Orlandi G (2008) *J Am Chem Soc* 130:5216–5230
26. Tiago ML, Ismail-Beigi S, Louie SG (2005) *J Chem Phys* 122:094311
27. Yuan S, Dou Y, Wu W, Hu Y, Zhao J (2008) *J Phys Chem A* 112:13326–13334
28. Siewertsen R, Neumann H, Buchheim-Stehn B, Herges R, Nather C, Renth F, Temps F (2009) *J Am Chem Soc* 131:15594–15595
29. Pancur T, Renth F, Temps F, Harbaum B, Kruger A, Herges R, Nather C (2005) *Phys Chem Chem Phys* 7:1985–1990
30. Lu YC, Diau EW, Rau H (2005) *J Phys Chem A* 109:2090–2099
31. Ciminelli C, Granucci G, Persico M (2005) *J Chem Phys* 123:174317
32. Nonnenberg C, Gaub H, Frank I (2006) *ChemPhysChem* 7:1455–1461
33. Norikane Y, Tamaoki N (2006) *Eur J Org Chem* 206:1296–1302
34. Janus K, Sworakowski J (2005) *J Phys Chem B* 109:93–101
35. Norikane Y, Katoh R, Tamaoki N (2008) *Chem Commun*: 1898–1900
36. Haberhauer G, Kallweit C (2010) *Angew Chem Int Ed* 49:2418–2421
37. Liu Z, Lu GY, Ma J (2011) *J Phys Org Chem* 24:568–577
38. Zhang CZ, Lu C, Zhu J, Lu GY, Wang X, Shi ZW, Liu F, Cui Y (2006) *Chem Mater* 18:6091–6093
39. Zhang CZ, Lu C, Zhu J, Wang CY, Lu GY, Wang CS, Wu DL, Liu F, Cui Y (2008) *Chem Mater* 20:4628–4641
40. Yang G, Su Z (2009) *Int J Quantum Chem* 109:1553–1559
41. Modelli A, Burrow PD (2009) *Phys Chem Chem Phys* 11:8448–8455
42. Becke D (1993) *J Chem Phys* 98:5648–5652
43. Lee C, Yang W, Parr RG (1988) *Phys Rev B* 37:785–789
44. Frisch MJ, Trucks GW, Schlegel HB, Scuseria GE, Robb MA, Cheeseman JR, Montgomery JA Jr, Vreven T, Kudin KN, Burant JC, Millam JM, Iyengar SS, Tomasi J, Barone V, Mennucci B, Cossi M, Scalmani G, Rega N, Petersson GA, Nakatsuji H, Hada M, Ehara M, Toyota K, Fukuda R, Hasegawa J, Ishida M, Nakajima T, Honda Y, Kitao O, Nakai H, Klene M, Li X, Knox JE, Hratchian HP, Cross JB, Bakken V, Adamo C, Jaramillo J, Gomperts R, Stratmann RE, Yazyev O, Austin AJ, Cammi R, Pomelli C, Ochterski JW, Ayala PY, Morokuma K, Voth GA, Salvador P, Dannenberg JJ, Zakrzewski VG, Dapprich S, Daniels AD, Strain MC, Farkas O, Malick DK, Rabuck AD, Raghavachari K, Foresman JB, Ortiz JV, Cui Q, Baboul AG, Clifford S, Cioslowski J, Stefanov BB, Liu G, Liashenko A, Piskorz P, Komaromi I, Martin RL, Fox DJ, Keith T, Al-Laham MA, Peng CY, Nanayakkara A, Challacombe M, Gill PMW, Johnson B, Chen W, Wong MW, Gonzalez C, Pople JA (2004) *Gaussian 03*. Gaussian Inc, Wallingford
45. Bouwstra JA, Schouten AJ (1983) *Acta Crystallogr C* 39:1121–1123
46. Traetteberg M, Hilmo I, Hagen K (1977) *J Mol Struct* 39:231–239
47. Tsuji T, Takashima H, Takeuchi H, Egawa T, Konaka S (2001) *J Phys Chem A* 105:9347–9353
48. Kurita N, Tanaka S, Itoh S (2000) *J Phys Chem A* 104:8114–8120
49. Ingold CK, Ingold EH (1926) *J Chem Soc*: 1310–1328
50. Biswas N, Umaphathy S (2000) *J Phys Chem A* 104:2734–2745
51. Friedl Z, Hapala H, Exner O (1979) *Collect Czech Chem Commun* 44:2928–2945
52. Lewis GN (1923) *Valence and structure of atoms and molecules*. Chemical Catalog Co, New York
53. McDaniel DH, Brown HC (1958) *J Org Chem* 23:420–427
54. Brown HC, Okamoto Y (1958) *J Am Chem Soc* 80:4979–4987
55. Biggs AI, Robinson RA (1961) *J Chem Soc*: 388–393
56. Kanis DR, Ratner MA, Marks TJ (1992) *J Am Chem Soc* 114:10338–10357
57. Meyers F, Marder SR, Pierce BM, Brédas JL (1994) *J Am Chem Soc* 116:10703–10714
58. Bourhill G, Brédas JL, Cheng LT, Marder SR, Meyers F, Perry JW, Tiemann BG (1994) *J Am Chem Soc* 116:2619–2620